Title

Coating nanoparticles with gastric epithelial cell membrane for targeted antibiotic delivery against Helicobacter pylori infection.

Journal

Advanced Therapeutics, 1(2)

Authors

Angsantikul, Pavimol
Thamphiwatana, Soracha
Zhang, Qiangzhe
et al.

Publication Date

2018-06-01

DOI

10.1002/adtp.201800016

Peer reviewed

HHS Public Access

Author manuscript

Adv Ther (Weinh). Author manuscript; available in PMC 2019 June 01.

Published in final edited form as:

Adv Ther (Weinh). 2018 June ; 1(2): . doi:10.1002/adtp.201800016.

Coating nanoparticles with gastric epithelial cell membrane for targeted antibiotic delivery against *Helicobacter pylori* infection

Pavimol Angsantikul,
Department of NanoEngineering and Moores Cancer Center, University of California San Diego, La Jolla, CA 92093, USA

Dr. Soracha Thamphiwatana,
Department of NanoEngineering and Moores Cancer Center, University of California San Diego, La Jolla, CA 92093, USA

Qiangzhe Zhang,
Department of NanoEngineering and Moores Cancer Center, University of California San Diego, La Jolla, CA 92093, USA

Kevin Spiekermann,
Department of NanoEngineering and Moores Cancer Center, University of California San Diego, La Jolla, CA 92093, USA

Jia Zhuang,
Department of NanoEngineering and Moores Cancer Center, University of California San Diego, La Jolla, CA 92093, USA

Dr. Ronnie H. Fang,
Department of NanoEngineering and Moores Cancer Center, University of California San Diego, La Jolla, CA 92093, USA

Dr. Weiwei Gao,
Department of NanoEngineering and Moores Cancer Center, University of California San Diego, La Jolla, CA 92093, USA

Prof. Marygorret Obonyo, and
Department of Medicine, University of California San Diego, La Jolla, CA 92093, USA

Prof. Liangfang Zhang
Department of NanoEngineering and Moores Cancer Center, University of California San Diego, La Jolla, CA 92093, USA

Abstract

Inspired by the natural pathogen-host interactions and adhesion, this study reports on the development of a novel targeted nanotherapeutics for the treatment of *Helicobacter pylori* (*H. pylori*) infection. Specifically, plasma membranes of gastric epithelial cells (e.g. AGS cells) are

Correspondence to: Marygorret Obonyo; Liangfang Zhang.

Conflict of Interest

The authors declare no conflict of interest.

collected and coated onto antibiotic-loaded polymeric cores, the resulting biomimetic nanoparticles (denoted AGS-NPs) bear the same surface antigens as the source AGS cells and thus have inherent adhesion to *H. pylori* bacteria. When incubated with *H. pylori* bacteria *in vitro*, the AGS-NPs preferentially accumulate on the bacterial surfaces. Using clarithromycin (CLR) as a model antibiotic and a mouse model of *H. pylori* infection, the CLR-loaded AGS-NPs demonstrate superior therapeutic efficacy as compared the free drug counterpart as well as non-targeted nanoparticle control group. Overall, this work illustrates the promise and strength of using natural host cell membranes to functionalize drug nanocarriers for targeted drug delivery to pathogens that colonize on the host cells. As host-pathogen adhesion represents a common biological event for various types of pathogenic bacteria, the bioinspired nanotherapeutic strategy reported here represents a versatile delivery platform that may be applied to treat numerous infectious diseases.

TOC image

An active targeting approach is reported for effective antibiotic delivery to *Helicobacter pylori* bacteria by mimicking and leveraging the natural pathogen-host binding interactions. Specifically, gastric epithelial cell membrane is collected and cloaked onto antibiotic-loaded polymeric nanoparticles. The resulting biomimetic nanotherapeutics show superior bactericidal effect *in vitro* and significantly reduce bacterial burden in a mouse model of *H. pylori* infection.

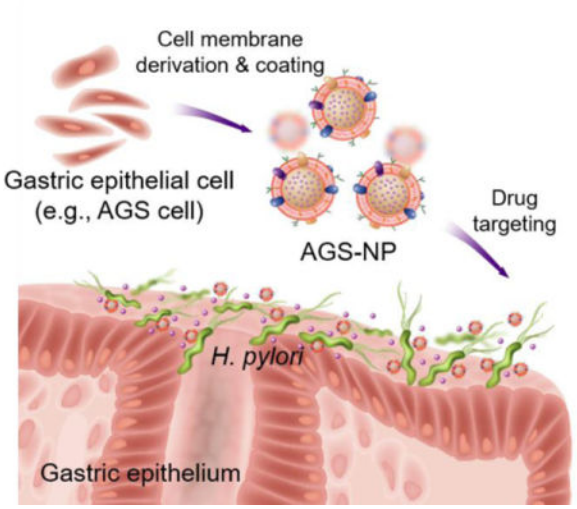

Keywords

nanomedicine; biomimetic nanoparticle; bacterial infection; antimicrobial delivery; active targeting

Introduction

Helicobacter pylori (*H. pylori*) is one of the most prevalent bacterial pathogens that infects more than half of the human population.[1, 2] *H. pylori* infection has been considered the major cause responsible for peptic ulcer disease, inflammatory gastritis, and gastric cancer, posing a significant healthcare burden worldwide.[3, 4] Currently, triple therapy based on

clarithromycin (CLR) in combination with a proton pump inhibitor (PPI) and an antibiotic (either amoxicillin or metronidazole) is the recommended treatment for *H. pylori* infection. However, mutations in *H. pylori* has led to resistance to CLR and other macrolides, causing a large number of treatment failures.[5] Meanwhile, resistance to other antibiotics including amoxicillin, metronidazole, and levofloxacin, is also rising rapidly. As a result, *H. pylori* eradication rates with standard triple therapy have declined significantly.[6, 7] Alternative agents and treatment regimens to address resistance development are being actively studied, but the results remain mixed.[8, 9] Clearly, new and effective anti-*H. pylori* treatments are urgently needed.

Unmet clinical needs in controlling *H. pylori* infection has prompted the development of anti-*H. pylori* nanoparticles with distinct therapeutic advantages. For example, nanoparticles have been made to encapsulate multiple antibiotics for concurrent delivery.[10, 11] With better controls over antibiotic release kinetics, the nanotherapeutics were able to minimize resistance development through additive or synergistic drug actions. Meanwhile, nanoparticles responsive to pH changes in the stomach or enzymatic activities have been developed.[12–14] They increased drug potency by only releasing drug payloads in the proximity of *H. pylori* infectious site Meanwhile, nanoparticles have also been conjugated with targeting ligands such as mannose-specific or fucose-specific lectins to target the carbohydrate receptors on *H. pylori* bacteria.[15] These targeted nanoparticles offered site-specific release and gastro-retentive properties, which together boosted local drug levels for a higher bactericidal efficacy. More recently, novel liposomes containing free fatty acids, which were prone to fusion with *H. pylori* bacteria, have been developed.[16, 17] These liposomes disrupted bacterial membrane and compromised the structural integrity of the bacteria for bioactivity, and thus showed a much lower rate to elicit drug resistance compared to conventional antibiotics.[18]

While therapeutic nanoparticles are increasingly applied to treat *H. pylori* infection, technologies for nanoparticle engineering and functionalization have also advanced significantly.[19–21] In particular, using natural cell membranes to coat nanoparticles has recently gained much attention. This strategy combines natural cell membranes with synthetic nanomaterials to leverage native cell functions for therapeutic applications.[22] One area is to harness the natural adhesion property of the source cells for targeted drug delivery.[23] For example, nanoparticles coated with cancer cell membranes inherited homotypic adhesion and showed an innate ability to bind with source cells for drug targeting.[24] In addition, nanoparticles coated with platelet membranes were shown to mimic the binding of platelets with pathogens such as methicillin-resistant *Staphylococcus aureus* for targeted antibiotic delivery.[25] Meanwhile, platelets also recognize tumor cells including circulating tumor cells through ligand binding interactions. Therefore, platelet membrane-coated nanoparticles were also developed for site-specific delivery of anticancer drugs.[26] These compelling applications inspire us to develop cell membrane-coated nanoparticles for targeted antibiotic delivery against *H. pylori* infection.

The adherence of *H. pylori* in the stomach is a pre-requisite for the bacteria to establish persistent infection.[27] Specifically, *H. pylori* bacteria display a preferential affinity through adherence pedestals to gastric epithelial cells of the gastric antrum. Various surface receptors

on gastric epithelial cells have been identified as receptors for *H. pylori* binding. For example, *H. pylori* were shown to bind with integrin β1 (CD29) in gastric epithelia cells.[28, 29] An increased expression of CD29 correlated with enhanced invasion of the bacteria. In addition, the fucosylated Lewis blood group antigens (Leb) on gastric epithelia cells are also known as receptors for *H. pylori* binding mediated through bacterial adhesin BabA.[30, 31] Furthermore, *H. pylori* is also known to gain adhesion through defined members of the carcinoembryonic antigen-related cell adhesion molecules (CEACAMs) on gastric epithelial cells via HopQ for adherence and subsequent translocation of cytotoxin-associated gene A (CagA) for virulence.[32]

Based on these adhesion mechanisms, we hypothesize that drug-loaded nanoparticles coated with plasma membranes derived from gastric epithelial cells will inherit the native pathogen-host adhesion and therefore are capable of *H. pylori* targeting. Herein, we derived membranes from AGS cells, a model gastric epithelia cell line, and coated them onto polymeric cores made from poly(lactic-co-glycolic acid) (PLGA, Figure 1). The resulting AGS membrane-coated nanoparticles (denoted 'AGS-NPs') present an external membrane coating for bacterial targeting and an internal polymeric core for drug encapsulation and controlled release. We further loaded AGS-NPs with CLR and demonstrated an enhanced bactericidal effect *in vitro* attributable to preferential binding of AGS-NPs with *H. pylori*. In a mouse model of *H. pylori* infection, CLR-loaded AGS-NPs showed superior anti-*H. pylori* efficacy when compared to free CLR or a non-targeted nanoparticle formulation. Overall, we demonstrated that AGS-NP formulation was effective in delivering antibiotics to *H. pylori* bacteria in an actively targeting manner and thus achieved high therapeutic efficacy.

Results and Discussion

The formulation process of AGS-NPs consists of three steps. In the first step, cytoplasm membranes of AGS cells were derived based on a previously established process, which involves hypotonic lysis, mechanical disruption, and differential centrifugation.[24, 33] In the second step, polymeric cores of PLGA were synthesized with a nanoprecipitation method, where acetone solution containing PLGA was added dropwise to an aqueous phase followed by evaporation. The nanoprecipitation process also allows for encapsulation of dye molecules or antibiotics by co-dissolving these molecules with PLGA in acetone. In the third step, AGS cell membranes were fused onto PLGA cores by mixing the cores with AGS membrane followed by sonication. Following the synthesis, dynamic light scattering (DLS) measurements on AGS-NPs showed that the diameter of the nanoparticles increased from 85.8 ± 4.4 nm of the PLGA cores to 102.2 ± 4.0 nm after the cell membrane coating (Figure 2A). Meanwhile, the surface zeta-potential increased from −41.5 ± 2.0 to −25.5 ± 3.3 mV. An increase of approximate 16 nm of nanoparticle diameter and a change of about 20 mV of the surface zeta-potential are attributable to the addition of a bilayer membrane onto the exterior of the PLGA cores.[24, 33] Following the fabrication, AGS-NPs were also examined under transmission electron microscopy (TEM) for morphology. Under the microscope, AGS-NPs present a typical core-shell structure, where a spherical core is surrounded by a unilamellar membrane coating (Figure 2B). AGS-NPs were suspended in water or 1X PBS and monitored for hydrodynamic sizes measured with DLS for 24 h. Herein, 1X PBS was used to simulate the pH level of stomach fluid when proton pump inhibitor (PPI) was

administered in subsequent anti-*H. pylori* treatment.[17] In PBS, AGS-NPs maintained stable sizes comparable to those in water, indicating an enhanced colloidal stability due to the membrane coating (Figure 2C). AGS-NPs were further analyzed with Western blot for antigenic information (Figure 2D). Specifically, we verified the presence of key membrane proteins responsible for *H. pylori* binding, including CD29 (integrin beta 1), blood group Lewis b (Leb), and CD66e (carcinoembryonic antigen-related cell adhesion molecule-5 or CEACAM5). Compared to cell lysate, membrane derivation also enriched membrane protein concentration, reflected by higher protein immunoblot intensity for AGS membrane vesicles (denoted AGS-vesicles) and AGS-NPs compared to that of the cell lysate. Overall, these results show the successful coating of AGS cell membranes onto polymeric cores.

After the nanoparticle synthesis, we tested the preferential targeting of AGS-NPs to *H. pylori* bacteria. As shown in Figure 3A, *H. pylori* (blue) showed a typical rod shape when observed under a fluorescence microscope. The image of the bacteria obtained with scanning electron microscopy (SEM) confirms the morphology and further reveals the polar sheathed flagella. Next, we mixed the bacteria with fluorescence-labeled AGS-NPs (red). The mixture was incubated at 37°C for 30 min. Following the incubation, the bacteria were thoroughly washed and then observed with a fluorescence microscope. In this case, sporadic red dots in the peripheral area of the bacteria were visible, suggesting AGS-NP retention and co-localization with the bacteria. Under SEM, the presence of individual nanoparticles on the bacteria was revealed, further verifying *H. pylori*–AGS-NP co-localization. To confirm AGS-NP targeting, we formulated polyethylene glycol (PEG)-coated PLGA nanoparticles (denote PEG-NPs), which are inert to bacterial binding, as a negative control. Although PEG-NPs were also fluorescence-labeled and had comparable sizes to AGS-NPs, they were not detected under either fluorescence microscope or SEM after incubation with the bacteria, therefore confirming the critical role played by AGS membrane coating for *H. pylori* targeting. We further quantified the overall fluorescence intensity of the bacterial samples. As shown in Figure 3B, *H. pylori* bacteria incubated with AGS-NPs showed a nearly 10-fold increase in fluorescence intensity compared to that of the bacteria incubated with PEG-NPs, confirming the occurrence of a prominent binding between AGS-NPs and *H. pylori* bacteria.

After having confirmed the preferential binding between AGS-NPs and *H. pylori* bacteria, we proceeded to examine whether AGS-NPs could carry CLR, one of the first-line antibiotics in anti-*H. pylori* treatment, and specifically deliver CLR to *H. pylori*. In the study, drug loading was achieved by co-dissolving CLR with PLGA polymer in acetone at desired ratios prior to nanoprecipitation. Following evaporation of the organic solvent, the cores were coated with AGS membrane, resulting in CLR-loaded AGS-NP (denoted AGS-NP(CLR)). In the study, we fixed PLGA amount and varied the initial CLR input from 0 to 30 w/w% of the polymer weight, a range where the resulting PLGA cores maintained comparable sizes and stability. As shown in Figure 4A, CLR loading yield increased when drug initial input was increased. The highest CLR loading yield of 12.43 ± 0.98% was achieved when drug initial input was kept at 30 w/w%. We selected this formulation for the following studies. Following drug loading, samples of free CLR and CLR released from AGS-NP(CLR) were analyzed with high performance liquid chromatography (HPLC). As shown in Figure 4B, CLR molecules released from nanoparticles elute at the same time as that of free CLR and peak shapes of the both are similar, suggesting that drug encapsulation

and membrane coating did not cause drug degradation. The release kinetics of CLR from AGS-NPs or bare PLGA cores were also examined (Figure 4C). The study was carried out in 1X PBS to simulate the pH level in stomach when PPI was applied to block gastric acid production.[17] Without membrane coating, PLGA cores showed a prominent burst release of CLR. In contrast, burst release was minimized when release from AGS-NP(CLR) was measured. In addition, CLR release rate from AGS-NPs stayed lower than that from uncoated PLGA cores. Specifically, a cumulative 83% of CLR was release from PLGA cores in 24 h, whereas only 68% was released from AGS-NP(CLR). A more prolonged drug release from AGS-NP(CLR) is likely due to the coated membranes, which acts as a barrier for drug diffusion out of the polymer matrix.[34]

After successful loading of CLR into AGS-NP, we next investigated the bactericidal activity of AGS-NP(CLR) against *H. pylori*. In the study, *H. pylori* was first incubated with free CLR, AGS-NP(CLR), or CLR-loaded PEG-NP (denoted PEG-NP(CLR)), followed by washing to remove free CLR and unbound PEG-NP(CLR), respectively. Bacteria were then cultured and enumerated. As shown in Figure 4D, under the experimental conditions, neither free CLR nor PEG-NP(CLR) was able to eradicate *H. pylori* bacteria. In contrast, bacteria incubated with AGS-NP(CLR) showed a nonlinear correlation between bacterial viability and nanoparticle concentrations. A drastic enhancement in bacterial killing of AGS-NP(CLR) compared to control formulations demonstrated a superior antibiotic targeting effect. For this study, we defined minimal bactericidal concentration (MBC) as the minimum concentration of the bactericidal agent required to kill 3 logs (99.9%) of the bacteria during a 30-min incubation. Accordingly, the value of MBC of AGS-NP(CLR) was determined to be 4 μg/mL.

Next, we evaluated the *in vivo* therapeutic efficacy of AGS-NP(CLR) against *H. pylori*. To this end, we first established a mouse model of infection with *H. pylori* SS1 strain.[35, 36] Specifically, we administered each C57BL/6 mouse with 3×10^8 CFU bacteria through oral gavage once every two days for four times (Figure 5A). After bacterial administration, infection was allowed to develop for two weeks and then infected mice were randomly divided into four groups (n=8 for each group) and treated with PBS, free CLR, PEG-NP(CLR), or AGS-NP(CLR). In the study, a CLR dosage of 30 mg/kg body weight was chosen based on existing studies.[37, 38] To avoid potential drug degradation, all mice were given proton pump inhibitor through oral gavage 30 min prior to the administration of all formulations to neutralize gastric acid in the stomach. Each formulation was administered once a day for five consecutive days. On day 6, mice were sacrificed and stomach tissues were processed for bacterial quantification. Therapeutic efficacy was evaluated by enumerating and comparing *H. pylori* colonies. As shown in Figure 5B, mice treated with PBS showed a high bacterial burden of 1.58×10^5 CFU/g of stomach tissue. Meanwhile, mice treated with free CLR and PEG-NP(CLR) carried a bacterial burden of 5.01×10^4 and 6.45×10^3 CFU/g of stomach tissue, respectively. These values correspond to a bacterial reduction of approximately 0.53 and 1.43 orders of magnitude, respectively. In contrast, the bacterial burden in mice treated with AGS-NP(CLR) was found to be 1.46×10^2 CFU/g of stomach tissue, approximately 3.08 orders of magnitude reduction. The superior anti-*H. pylori* efficacy found with AGS-NP(CLR) demonstrates the effectiveness of AGS membrane coating for drug targeting.

Lastly, we evaluated the toxicity of AGS-NP with uninfected C57BL/6 mice. In the study, mice were orally administered with AGS-NP once daily for 5 consecutive days with the same dosing regimen as the one used in above efficacy study. Mice administered with PBS buffer were used as a control group. During the study, mice administered with AGS-NPs maintained the same body weight compared to mice administered with PBS and all mice showed stable body weight and steady growth (Figure 6A). On day 7, all mice were sacrificed and the longitudinal sections of gastric tissues obtained from the mice were collected and stained with hematoxylin and eosin (H&E). Under microscope, tissue samples of mice from both groups show clear layers of mucosa, muscularis mucosa, and submucosa (Figure 6B). When zoomed-in, the gastric tissues from mice treated with AGS-NPs maintained an undisturbed structure with a clear layer of epithelial cells and well-organized gastric pits, which was similar to the gastric samples treated with PBS only. The absence of any detectable gastric histopathologic changes or toxicity within a five-day treatment suggests that orally administered AGS-NPs is safe.

Targeted delivery can promote drug-pathogen localization and minimizes drug systemic exposure, therefore reducing the risk of drug resistance.[21] To achieve effective drug targeting, one common method is to conjugate nanoparticles with bacterium-specific ligands including small molecules, peptides, antibodies, and aptamers.[19] However, the application of such ‘bottom-up’ strategy may be limited by the availability of reliable ligands for pathogen binding as well as the robustness of the conjugation process. In contrast, cell membrane coating approach represents an alternative ‘top-down’ method that leverages native cell-pathogen adhesion mechanisms for targeting without ligand selection and conjugation. Like *H. pylori*, various opportunistic pathogens, such as strains of staphylococci, streptococci, and *Escherichia coli*, are also known to exploit complex adhesion mechanisms for host cell adhesion and colonization.[39, 40] Cell membrane coating is an effective approach to harnessing these biological mechanisms and replicate the binding. Using membranes from their host cells to coat nanoparticles is expected to be applicable for antibiotic targeting against the pathogen infections. In addition, harnessing patient’s host cell functions for pathogen targeting may open new opportunities to enable patient-specific and disease-specific precision medicine.[41]

In this study, we selected CLR as a model antibiotic to demonstrate the targeted delivery ability of the AGS-NPs. As PLGA nanoparticles have extensive applications in drug encapsulation and delivery, AGS-NPs are expected to load and deliver other antibiotics or antibiotic combinations to further improve anti-*H. pylori* efficacy.[42] Herein, AGS-NPs are designed with a diameter of approximately 100 nm and a negative surface charge, as nanoparticles with a comparable size and surface charge are known to effectively penetrate mucus layer.[17, 43] In addition, blank cell membrane-coated PLGA nanoparticles (without drugs) are known to neutralize bacterial toxins for antivirulence therapy[44, 45]. Similar toxin decoy effect may also exist for the AGS-NPs against *H. pylori* bacteria.[17] Meanwhile, nanoparticle cores made with materials such as mesoporous silica, macromolecule gelatin, and cross-linked acrylamide have been coated with cell membranes.[22] New coating processes, such as cell membrane vesicle-templated in situ gelation, have also been developed.[46] Furthermore, the future development of AGS-NPs toward clinical use needs to address cell membrane supply issue. In this regard, the rapid development of *ex vivo* cell

expansion technology may be able to supply sufficient amount of cell membrane materials for clinical studies.[47, 48] Meanwhile, the well-established genetic engineering approaches would allow for on-demand cell membrane modification for specific functions and uses.[49] The advancement of these technologies together would offer a promising prospect to the translation of AGS-NPs and the cell membrane-coating technology in general.

These technological advances can be also applied to enable new antimicrobial strategies beyond antibiotic delivery. For instance, cell membrane-coated nanoparticles have been developed to neutralize bacterial toxins based on toxins' virulent mechanisms rather than their structures, therefore enabling broad-spectrum and 'drug free' antivirulence therapy.[50, 51] As another 'drug free' strategy to combat infection, cell membrane-coated nanoparticles have also been developed as antibacterial vaccines. In this case, nanoparticles coated with bacterial outer membranes not only present the natural antigen presentation by bacteria to the immune system, but also modulate the host immune response through size-controlled lymphatic targeting. Meanwhile, bacterium-secreted virulent toxins have been entrapped using cell membrane-coated nanoparticles, resulting in multivalent nanotoxoids capable of delivering diverse virulence factors in a natural, concurrent, and safe fashion for immunity.[52, 53] The nanotoxoid formulation consistently outperformed traditional vaccine formulations prepared from denatured proteins. Overall, these developments illustrate the promise and strength of using cell membrane coating technology to address the therapeutic challenges of bacterial infections.

Conclusions

In summary, we derived natural membranes of AGS cells, a gastric epithelial cell line, and coated them onto PLGA polymeric cores. The resulting AGS-NPs preserved cell surface antigens used by *H. pylori* bacteria to adhere and colonize the host. AGS-NPs showed preferential binding and retention with *H. pylori* when compared to control nanoparticles coated with synthetic PEG. We further loaded CLR into AGS-NPs and achieved high drug loading yield and prolonged drug release profile from the nanoparticles. The resulting CLR-loaded AGS-NPs showed superior bactericidal effect *in vitro* and were able to effectively reduce bacterial burden in a mouse model of *H. pylori* infection. In addition, mouse body weight and stomach histology in a toxicity test showed no adverse effects from the AGS-NPs. Collectively, these results demonstrate that AGS-NPs are an effective and safe approach for targeted antibiotic delivery to treat *H. pylori* infection.

Experimental section

AGS cell culture and membrane derivation

AGS cell line (human gastric adenocarcinoma, ATCC CRL-1739) was purchased from the American Type Culture Collection (ATCC) and maintained in Ham F-12K Medium (Invitrogen) supplemented with 10% fetal bovine serum (FBS, Hyclone) and 1% penicillin-streptomycin (100 U/mL penicillium and 100 μg/mL streptomycin, Invitrogen) at 37°C in a humidified atmosphere containing 5% CO_2. For cell membrane derivation, AGS cells were grown in T-175 culture flasks to 70-80% confluency and detached with 2 mM ethylenediaminetetraacetic acid (EDTA, USB Corporation) in phosphate buffered saline

(PBS, Invitrogen) and washed in PBS three times by centrifuging at 500 × g for 10 min. The pellet was suspended in homogenization buffer (HB) consisting of 75 mM sucrose, 20 mM Tris-HCl pH 7.5 (Mediatech), 2 mM $MgCl_2$ (Sigma Aldrich), 10 mM KCl (Sigma Aldrich), and protease/phosphatase inhibitors cocktails. Cells were disrupted by a dounce homogenizer (20 passes), then spun down at 3,200 × g for 5 min. The supernatant was saved while the pellet was resuspended in HB and the homogenization and centrifugation were repeated again. The supernatants were pooled and centrifuged at 7,600 × g for 25 min, after which the pellet was discarded and the supernatant was centrifuged at 29,600 × g for 35 min. The supernatant was discarded and the pellet was resuspend in 10 mM Tris-HCl pH = 7.5 and 1 mM EDTA and centrifuged again at 29,600 × g for 35 min. The pellet containing the plasma membrane material was then collected and resuspended in DI water. Samples were aliquoted and stored in −80°C fridge for subsequent studies.

Nanoparticle synthesis and characterization

To synthesize polymeric nanoparticle cores, 0.67 dl/g acid (carboxyl)-terminated 50:50 poly (lactic-co-glycolic acid) (PLGA, molecular weight: ~44 kDa, polydispersity: ~2) (LACTEL Absorbable Polymers) in acetone was nanoprecipitated in aqueous solution. To prepare fluorescently labeled PLGA cores, 1,19-dioctadecyl-3,3,3′,3′-tetramethylindodicarbocyanine perchlorate (DiD, $\lambda_{excitation/emission}$ = 644/665 nm, 0.1 wt%, Life Technologies) was dissolved together with PLGA in acetone followed by the nanoprecipitation process. The nanoparticle solution was then put under vacuum to remover organic solvent with continuous stirring for 2h. To synthesize AGS cell membrane-coated nanoparticles (AGS-NPs), PLGA nanoparticles cores were mixed with membrane vesicles at 1:2 membrane protein to polymer weight ratio, and sonicated using a bath sonicator (FS30D, Fisher Scientific, with a frequency of 42 kHz and a power of 100 W for 5 min) to coat membranes on to polymeric cores. Following the coating, AGS-NPs were purified by centrifugation at 16,000× g for 10 mins to remove unbound membrane fragments. AGS membrane-derived vesicles (AGS-vesicles) were prepared by sonicating collected cell membranes without PLGA cores for 2 min. As a control group, PLGA nanoparticles coated with polyethylene glycol (PEG-NPs) were fabricated through a nanoprecipitation method previously described. Briefly, a solution of PLGA in acetone was nanoprecipitated into an aqueous phase containing 1,2-distearoyl-sn-glycero-3-phosphoethanolamine-N-[methoxy(polyethylene glycol)-2000] (DSPE-mPEG2000, average Mw = 2.8 kDa, Laysan Bio, Inc., AL, 10 wt% of PLGA). The nanoparticle solution was then placed under vacuum to remover organic solvent with continuous stirring for 2h.

Following the nanoparticle synthesis, dynamic light scattering (DLS) studies were performed to measure the hydrodynamic size and surface zeta potential (Malvern ZEN 3600 Zetasizer). All measurements were carried out in triplicate at room temperature. To examine the nanoparticle miscroscopic morphology, AGS-NP samples were visualized with transmission electron microscopy (TEM, Tecnai G2 Sphera FEI 200 kV). Briefly, AGS-NP samples (1 mg/mL) were dropped onto carbon-coated copper grid and left for 1 min, and then washed off with DI water. The sample was then stained with 1 wt% uranyl acetate (Sigma Aldrich) before imaging.

Membrane protein characterization

An SDS-PAGE assay (Thermo Fisher Scientific) was carried out to examine the protein profile of AGS cell lysates, AGS membranes, and AGS-NPs. Specifically, all samples were adjusted to equivalent total protein concentrations in lithium dodecyl sulfate (LDS) loading buffer. The samples were then separated on a 4–12% Bis-Tris 17-well minigel in MOPS running buffer using a Novex Xcell SureLock Electrophoresis System. The protein bands were stained with InstantBlue Protein Stain (Expedeon) for observation according to manufacturer's protocol. Western blotting was conducted to identify membrane proteins on AGS-NPs. Specifically, gels from the SDS-PAGE study were transferred onto a nitrocellulose membranes (Thermo Scientific) and probed with primary antibodies including mouse anti-human CD29 (Biolegend), mouse anti-human Blood Group Lewis b (Santa Cruz Biotechnology), and mouse anti-human CD66e (CEACAM5, Santa Cruz Biotechnology). Horseradish peroxidase (HRP)-conjugated secondary antibodies including goat anti-mouse IgG (Biolegend) and goat anti-mouse IgM (Southern Biotech) were used as secondary staining based on the isotype of the primary antibodies. The nitrocellulose membrane was then incubated with ECL western blotting substrate (Pierce) and developed with the Mini-Medical/90 Developer (ImageWorks).

AGS-NP targeting to H. pylori bacteria

H. pylori Sydney strain 1 (SS1) was maintained on Columbia agar supplemented with 5% horse blood (Hardy Diagnostics) at 37°C under microaerobic conditions (10% CO_2, 85% N_2, and 5% O_2). Before the experiments, a single colony of *H. pylori* from the agar plate was inoculated into Brain Heart Infusion (BHI) broth containing 5% FBS and incubated overnight at 37°C under microaerobic conditions with moderate reciprocal shaking. Following the culture, the bacteria were harvested by centrifugation at 5,000 × g for 10 min, washed with sterile 1X PBS twice, and suspended to a concentration of 1×10^8 CFU/mL (OD_{600} = 1.0) in PBS. For the targeting study, 500 μL of *H. pylori* SS1 (5×10^7 CFU) was added with 200 μL DiD-labeled AGS-NPs or PEG-NPs (250 μg/mL in 1X PBS) and the samples were allowed to mix for 30 min at room temperature. Unbound nanoparticles were removed from the bacteria by repeated centrifugal and washing steps (5,000 × g and 1X PBS). The bacteria were then suspended in 1X PBS and fixed with 2% glutaraldehyde (Sigma Aldrich) for 2 h at room temperature. For imaging by deconvolution scanning fluorescence microscope (DeltaVision System, Applied Precision), post-fixed bacterial suspension was mixed at 1:1 ratio with Vectashield mounting medium containing DAPI. Then 5 μL of the bacterial suspension was dropped on a poly-L-lysine coated glass slide, sealed with coverslip and the fluorescence images were obtained. To quantify DiD fluorescence intensity, bacterial samples were added to a 96-well plate and read with a plate reader (Biotek Spectroscopy). AGS-NP targeting to *H. pylori* was also observed with scanning electron microscopy (SEM, FEI/Philips XL30 ESEM). Briefly, 5 μL of the post-fixed bacterial suspension was dropped onto a polished silicon wafer and allowed to dry overnight in a biosafety cabinet. The sample was then coated with chromium and imaged. In all experiments, bacterial sample without adding the nanoparticles was used as a control.

Drug loading and release studies

To load clarithromycin (CLR) into AGS-NPs, CLR and PLGA were mixed and dissolved in acetone, followed by precipitation into water containing 1 wt% of F68 (Invitrogen). Solutions were stirred for 4 h to evaporate the organic solvent. Loading efficiency was studied by varying the weight ratio of CLR to PLGA from 5 to 30 wt%. Following the preparation, nanoparticles were washed with Amicon Ultra-4 centrifugal filters (Millipore, 10 kDa cut-off) and then used for membrane coating as described above. To measure CLR loading yield, 1 mL of AGS-NPs (6 mg/mL) was lyophilized. Dried AGS-NPs were first dissolved in 200 μL acetronitrile, and then added with 200 μL methanol to extract CLR. Samples were then centrifuged at 21,000 × g. The supernatants were collected and the pellets were discarded. The concentration of CLR in the supernatant samples was measured by high performance liquid chromatography (HPLC, with a PerkinElmer Brownlee C18 analytical column, 4.6 × 100 mm, 3 μm particle size). The mobile phase contained methanol and 0.067 M monobasic potassium phosphate (13:7) and pH was adjusted to 4.0 with phosphoric acid. The flow rate was kept at 1.0 mL/min and the detector wavelength was set as 205 nm.

To study the release kinetics of CLR from AGS-NPs, the samples (6 mg/mL, 200 μL) were loaded into Slide-A-Lyzer mini dialysis devices (10K MWCO, Thermo Scientific Pierce) and then dialyzed against 2L of 1X PBS. PBS buffer was replaced every 12 h during the dialysis process. At each predetermined time point, AGS-NP solutions in three mini dialysis cups were collected and CLR concentration was measured as described above.

Bactericidal activity of CLR-loaded AGS-NPs against H. pylori

Bacteria were pelleted from liquid culture with centrifugation at 3000 × g for 7 min and resuspended in fresh BHI to a concentration of 5×10^7 CFU/mL. Then 200 μL of the bacterial solution was mixed with 1000 μL free CLR, CLR-loaded PEG-NPs, CLR-loaded AGS-NPs with a final drug concentration ranging from 0 to 8 μg/mL. Mixtures were first cultured at 37°C under microaerobic condition on reciprocal shaker for 30 min and then centrifuged at 3,000 × g for 7 min. Bacterial pellets were washed twice with PBS to remove unbound drugs and NPs and then resuspended with fresh BHI, followed by an overnight incubation. After the incubation, the samples were serial diluted 10 to 10^7-fold with 1X PBS. The bacterial suspensions were spotted onto Columbia agar plates with 5% laked horse blood. The agar plates were incubated for 3-5 days for bacterial enumeration.

Induction of H. pylori infection in mice

Six-week-old C57BL/6 male mice were purchased from the Jackson Laboratory (Bar Harbor, ME). Mice were housed in the Animal Facility at the University of California San Diego under federal, state, local, and National Institutes of Health guidelines for animal care. To induct infection, each C57BL/6 mouse received 0.3 mL of 1×10^9 CFU/mL *H. pylori* in BHI broth administered intragastrically through oral gavage every 48 h, repeated three times (on day 3, 5, and 7, respectively), and the infection was allowed to develop for 2 weeks.

In vivo anti-H. pylori efficacy of CLR-loaded AGS-NPs

Infected mice were randomly divided into four treatment groups (n=8) and orally administered with CLR-loaded AGS-NPs, CLR-loaded PEG-NPs, free CLR, (with 30 mg/kg CLR dosage) or PBS. Administration was performed once daily for 5 consecutive days. Before the treatment, mice were first administered with omeprazole (a proton pump inhibitor) through oral gavage at a dose of 400 μmol/kg body weight, followed by a lag time of 30 min before administration of different treatment groups. Forty-eight hours after last administration, mice were sacrificed and the stomachs were excised from the abdominal cavity. The stomachs were cut along the greater curvature, and the gastric content was removed. Stomach tissues were rinsed with 1X PBS and weighed. Then samples were suspended in 200 μL 1X PBS and homogenized with Bullet Blender homogenizer (Next Advance). The homogenate was serially diluted and spotted onto Columbia agar plate with 5% laked horse blood and Skirrow's supplement (10 μg/mL vancomycin, 5 μg/mL trimethoprim lactate, 2,500 IU/L polymyxin B, Oxiod). The plates were then incubated at 37°C under a microaerobic condition for 5 days and then bacterial colonies were enumerated.

Evaluation of AGS-NP toxicity in vivo

To evaluate the acute toxicity of the AGS-NPs *in vivo*, uninfected C57BL/6 male mice (n=6, 25–30 g each) were orally administered with AGS-NPs once daily for 5 consecutive days using the procedure as described above. Control mice were administered with PBS. During the experimental period, the mouse body weight was monitored daily. On day 6, mice were sacrificed and sections of the mouse stomach tissues were processed for histological examination. The stomach was cut open along the greater curvature, and the gastric content was removed. The longitudinal tissue sections were fixed in neutral-buffered 10 v/v% formalin for 15 h, transferred into 70% ethanol, and then embedded in paraffin. The tissue sections were cut with 5 μm thickness and stained with hematoxylin and eosin (H&E). The stained sections were visualized by Hamamatsu NanoZoomer 2.0HT and the images processed using NDP viewing software.

Statistical Analysis

DLS and plate reader data represent averaged values (obtained from 3 replicates) with standard deviation shown as error bars. For Western blot studies, the experiments were performed in triplicate and a representative image was shown. In fluorescence and SEM imaging, experiments were performed in triplicate and a representative image was shown. To examine the statistical significance, unpaired two-tailed t-tests were performed in GraphPad Prism 7 with confidence level $P = 0.05$ deemed significant.

Acknowledgments

This work is supported by the National Institutes of Health under Award Numbers R01DK095168 and R01CA200574.

References

1. O'Connor A, O'Morain CA, Ford AC. Nat Rev Gastroenterol Hepatol. 2017; 14:230. [PubMed: 28053340]
2. Salama NR, Hartung ML, Muller A. Nat Rev Microbiol. 2013; 11:385. [PubMed: 23652324]
3. Yamaoka Y. Nat Rev Gastroenterol Hepatol. 2010; 7:629. [PubMed: 20938460]
4. McColl KEL. New Engl J Med. 2010; 362:1597. [PubMed: 20427808]
5. Alba C, Blanco A, Alarcon T. Curr Opin Infect Dis. 2017; 30:489. [PubMed: 28704226]
6. Hu Y, Zhang M, Lu B, Dai JF. Helicobacter. 2016; 21:349. [PubMed: 26822340]
7. Zhang M. World J Gastroenterol. 2015; 21:13432. [PubMed: 26730153]
8. Georgopoulos SD, Papastergiou V, Karatapanis S. Expert Opin Pharmacother. 2015; 16:2307. [PubMed: 26330278]
9. Hu Y, Zhu Y, Lu NH. Front Cell Infect Microbiol. 2017; 7 article number 168.
10. Ramteke S, Ganesh N, Bhattacharya S, Jain NK. J Drug Targeting. 2009; 17:225.
11. Ramteke S, Jain NK. J Drug Targeting. 2008; 16:65.
12. Lin YH, Chang CH, Wu YS, Hsu YM, Chiou SF, Chen YJ. Biomaterials. 2009; 30:3332. [PubMed: 19299008]
13. Thamphiwatana S, Fu V, Zhu JY, Lu DN, Gao W, Zhang L. Langmuir. 2013; 29:12228. [PubMed: 23987129]
14. Thamphiwatana S, Gao W, Pornpattananangkul D, Zhang QZ, Fu V, Li JY, Li JM, Obonyo M, Zhang L. J Mater Chem B. 2014; 2:8201. [PubMed: 25544886]
15. Umamaheshwari RB, Jain NK. J Drug Targeting. 2003; 11:415.
16. Obonyo M, Zhang L, Thamphiwatana S, Pornpattananangkul D, Fu V, Zhang L. Mol Pharm. 2012; 9:2677. [PubMed: 22827534]
17. Thamphiwatana S, Gao W, Obonyo M, Zhang L. Proc Natl Acad Sci U S A. 2014; 111:17600. [PubMed: 25422427]
18. Jung SW, Thamphiwatana S, Zhang L, Obonyo M. PLoS One. 2015; 10 article number e0116519.
19. Gao W, Thamphiwatana S, Angsantikul P, Zhang L. Wiley Interdiscip Rev Nanomed Nanobiotechnol. 2014; 6:532. [PubMed: 25044325]
20. Kumar B, Jalodia K, Kumar P, Gautam HK. J Drug Deliv Sci Technol. 2017; 41:260.
21. Gao W, Chen Y, Zhang Yue, Zhang Q, Zhang Liangfang. Adv Drug Del Rev. 2018 in press.
22. Fang R, Kroll A, Gao W, Zhang L. Adv Mater. 2018 in press.
23. Gao W, Zhang L. J Drug Targeting. 2015; 23:619.
24. Fang RH, Hu CMJ, Luk BT, Gao W, Copp JA, Tai YY, O'Connor DE, Zhang L. Nano Lett. 2014; 14:2181. [PubMed: 24673373]
25. Hu CMJ, Fang RH, Wang KC, Luk BT, Thamphiwatana S, Dehaini D, Nguyen P, Angsantikul P, Wen CH, Kroll AV, Carpenter C, Ramesh M, Qu V, Patel SH, Zhu J, Shi W, Hofman FM, Chen TC, Gao W, Zhang K, Chien S, Zhang L. Nature. 2015; 526:118. [PubMed: 26374997]
26. Hu QY, Sun WJ, Qian CG, Wang C, Bomba HN, Gu Z. Adv Mater. 2015; 27:7043. [PubMed: 26416431]
27. Sgouras DN, Trang TTH, Yamaoka Y. Helicobacter. 2015; 20:8. [PubMed: 26372819]
28. Kaplan-Turkoz B, Jimenez-Soto LF, Dian C, Ertl C, Remaut H, Louche A, Tosi T, Haas R, Terradot L. Proc Natl Acad Sci U S A. 2012; 109:14640. [PubMed: 22908298]
29. Koelblen T, Berge C, Cherrier MV, Brillet K, Jimenez-Soto L, Ballut L, Takagi J, Montserret R, Rousselle P, Fischer W, Haas R, Fronzes R, Terradot L. FEBS J. 2017; 284:4143. [PubMed: 29055076]
30. Fei YY, Schmidt A, Bylund G, Johansson DX, Henriksson S, Lebrilla C, Solnick JV, Boren T, Zhu XD. Anal Chem. 2011; 83:6336. [PubMed: 21721569]
31. Parreira P, Shi Q, Magalhaes A, Reis CA, Bugaytsova J, Boren T, Leckband D, Martins MCL. J R Soc Interface. 2014; 11 article number 20141040.

32. Koniger V, Holsten L, Harrison U, Busch B, Loell E, Zhao Q, Bonsor DA, Roth A, Kengmo-Tchoupa A, Smith SI, Mueller S, Sundberg EJ, Zimmermann W, Fischer W, Hauck CR, Haas R. Nat Microbiol. 2017; 2 article number 16188.
33. Thamphiwatana S, Angsantikul P, Escajadillo T, Zhang QZ, Olson J, Luk BT, Zhang S, Fang RH, Gao W, Nizet V, Zhang L. Proc Natl Acad Sci U S A. 2017; 114:11488. [PubMed: 29073076]
34. Aryal S, Hu CMJ, Fang RH, Dehaini D, Carpenter C, Zhang DE, Zhang L. Nanomedicine. 2013; 8:1271. [PubMed: 23409747]
35. Obonyo M, Guiney DG, Harwood J, Fierer J, Cole SP. Infect Immun. 2002; 70:3295. [PubMed: 12011029]
36. Hase K, Murakami M, Iimura M, Cole SP, Horibe Y, Ohtake T, Obonyo M, Gallo RL, Eckmann L, Kagnoff MF. Gastroenterology. 2003; 125:1613. [PubMed: 14724813]
37. Jenks PJ, Ferrero RL, Tankovic J, Thiberge JM, Labigne A. Antimicrob Agents Chemother. 2000; 44:2623. [PubMed: 10991835]
38. van Zanten S, Kolesnikow T, Leung V, O'Rourke JL, Lee A. Antimicrob Agents Chemother. 2003; 47:2249. [PubMed: 12821476]
39. Fitzgerald JR, Foster TJ, Cox D. Nat Rev Microbiol. 2006; 4:445. [PubMed: 16710325]
40. Pizarro-Cerda J, Cossart P. Cell. 2006; 124:715. [PubMed: 16497583]
41. Zmora N, Zeevi D, Korem T, Segal E, Elinav E. Cell Host & Microbe. 2016; 19:12. [PubMed: 26764593]
42. Makadia HK, Siegel SJ. Polymers. 2011; 3:1377. [PubMed: 22577513]
43. Lai SK, Wang Y-Y, Hanes J. Adv Drug Del Rev. 2009; 61:158.
44. Wang F, Gao W, Thamphiwatana S, Luk BT, Angsantikul P, Zhang QZ, Hu CMJ, Fang RH, Copp JA, Pornpattananangkul D, Lu WY, Zhang L. Adv Mater. 2015; 27:3437. [PubMed: 25931231]
45. Zhang Y, Gao W, Chen YJ, Escajadillo T, Ungerleider J, Fang RH, Christman K, Nizet V, Zhang L. ACS Nano. 2017; 11:11923. [PubMed: 29116753]
46. Zhang JH, Gao W, Fang RH, Dong AJ, Zhang L. Small. 2015; 11:4309. [PubMed: 26044721]
47. Yu HY, Chen W, Li CL, Lin D, Liu JD, Yang ZE, Yang JG, Sun YH, Ma DC. Exp Ther Med. 2017; 14:5678. [PubMed: 29285110]
48. Lambrechts T, Sonnaert M, Schrooten J, Luyten FP, Aerts JM, Papantoniou I. Tissue Engineering Part B-Reviews. 2016; 22:485. [PubMed: 27333790]
49. Gee AP. Cancer Gene Ther. 2015; 22:67. [PubMed: 25633481]
50. Hu CMJ, Fang RH, Copp J, Luk BT, Zhang L. Nat Nanotechnol. 2013; 8:336. [PubMed: 23584215]
51. Chen Y, Chen M, Zhang Y, Lee JH, Escajadillo T, Gong H, Fang R, Gao W, Nizet V, Zhang L. Adv Healthc Mater. 2018 in press.
52. Hu CMJ, Fang RH, Luk BT, Zhang L. Nat Nanotechnol. 2013; 8:933. [PubMed: 24292514]
53. Wei XL, Gao J, Wang F, Ying M, Angsantikul P, Kroll AV, Zhou JR, Gao W, Lu WY, Fang RH, Zhang L. Adv Mater. 2017; 29 article number 1701644.

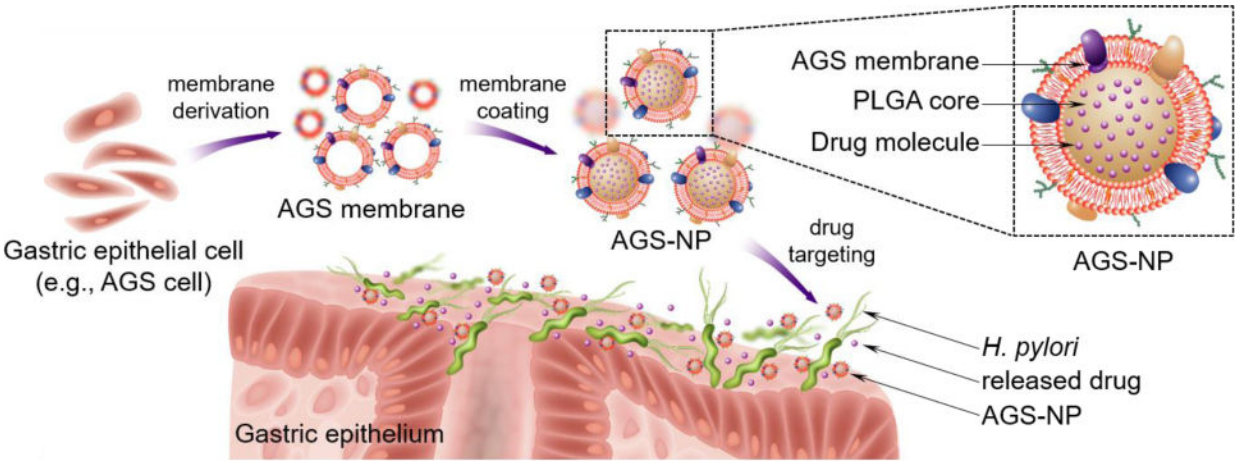

Figure 1.

Schematic illustrations of the preparation of gastric epithelial cell (e.g. AGS cell) membrane-coated nanoparticles (denoted 'AGS-NPs') and their use for targeted antibiotic delivery to treat *Helicobacter pylori* (*H. pylori*) infection. To prepare AGS-NPs, cellular membranes are first derived from AGS cells, a human stomach adenocarcinoma cell line. AGS-NPs are then fabricated by coating poly(lactic-co-glycolic acid) (PLGA) polymeric cores with AGS membranes, which contain key antigens for *H. pylori* binding. The resulting AGS-NPs mimic natural pathogen-host binding interactions. Following the administration into the stomach, the AGS-NPs are expected to preferentially bind with *H. pylori* bacteria and release antibiotic payload onsite for enhanced antibacterial efficacy.

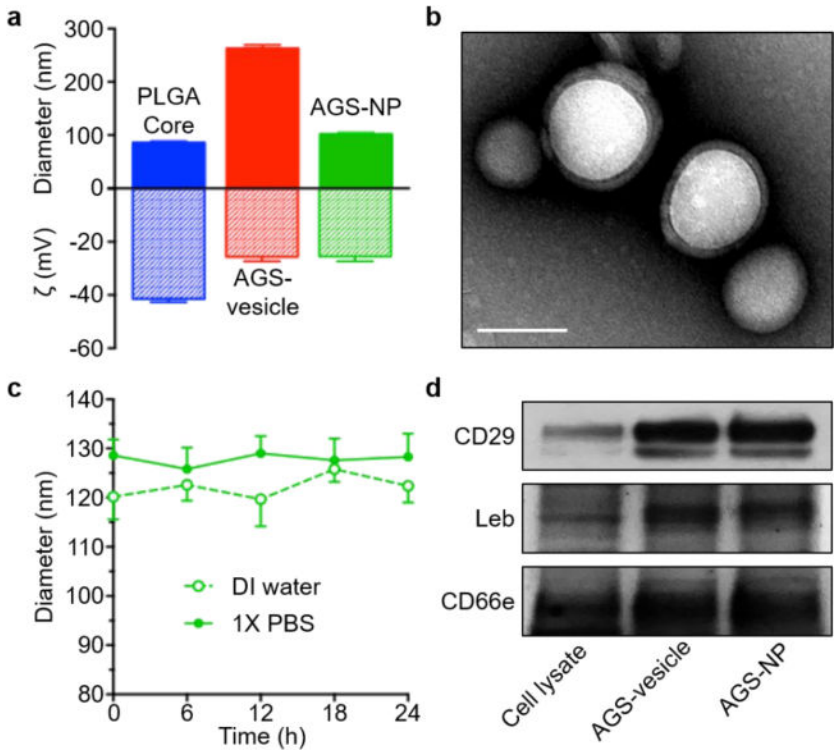

Figure 2.

Physicochemical characterization of AGS-NPs. (a) Dynamic light scattering (DLS) measurements of hydrodynamic size (diameter, nm) and surface zeta potential (ζ, mV) of PLGA cores, AGS membrane vesicles (AGS-vesicle), and AGS-NPs (n = 3). (b) Translation electron microscopy (TEM) image of AGS-NPs stained with uranyl acetate. Scale bar = 100 nm. (c) Stability of AGS-NPs in DI water or 1X PBS, determined by monitoring particle size (diameter, nm), over a span of 24 h (n=3). (d) Western blotting analysis for AGS membrane-specific protein markers. Samples were run at equal protein concentrations and immunostained against membrane markers including CD29, Leb, and CD66e. Experiments were performed in triplicate and a representative image was shown.

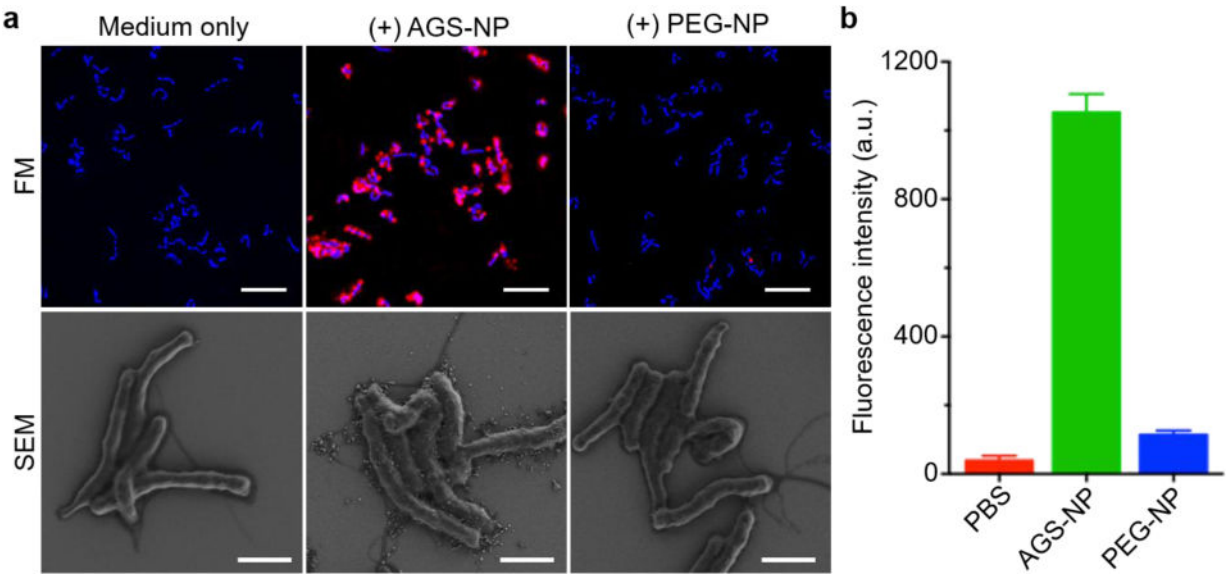

Figure 3.

AGS-NPs targeting to *H. pylori* bacteria (a) Fluorescence microscopy (FM, top row) and scanning electron microscopy (SEM, bottom row) images of *H. pylori* bacteria after incubation with medium only, AGS-NPs, and corresponding pegylated PLGA nanoparticles (PEG-NPs), respectively. Scale bar = 5 μm in FM and 1 μm in SEM, respectively. (b) Fluorescence intensity at 665 nm measured from the *H. pylori* bacterial samples incubated with PBS, AGS-NPs, and PEG-NPs, respectively. In FM images and fluorescent intensity measurements, AGS-NP and PEG-NP were labeled with DiD dye (red) and *H. pylori* were stained with DAPI (blue). Experiments of FM and SEM were performed in triplicate and a representative image was shown. Bars represent means ± SD (n = 3).

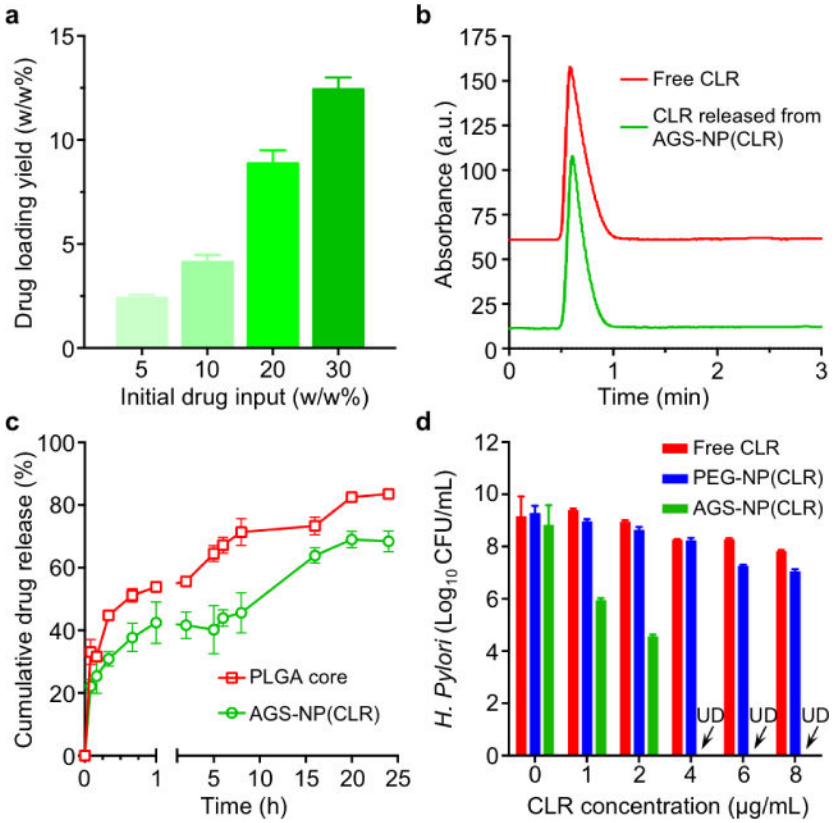

Figure 4.

Characterization of clarithromycin(CLR)-loaded AGS-NP (denoted 'AGS-NP(CLR)'). (a) Quantification of CLR loading yield of AGS-NP(CLR) when initial drug input was varied from 0 to 30 w/w%. (b) Chromatogram of free CLR and CLR released from AGS-NP(CLR). The flow rate was kept 1.0 mL/min and a detector wavelength at 205 nm. (c) CLR release profiles from PLGA core without membrane coating (red) and from AGS-NP(CLR). Data points represent means ± SD (n = 3). (d) *In vitro* bactericidal activity of free CLR, PEG-NP(CLR), and AGS-NP(CLR) against *H. pylori* bacteria, respectively. Bars represent means ± SD (n = 3). UD = undetectable.

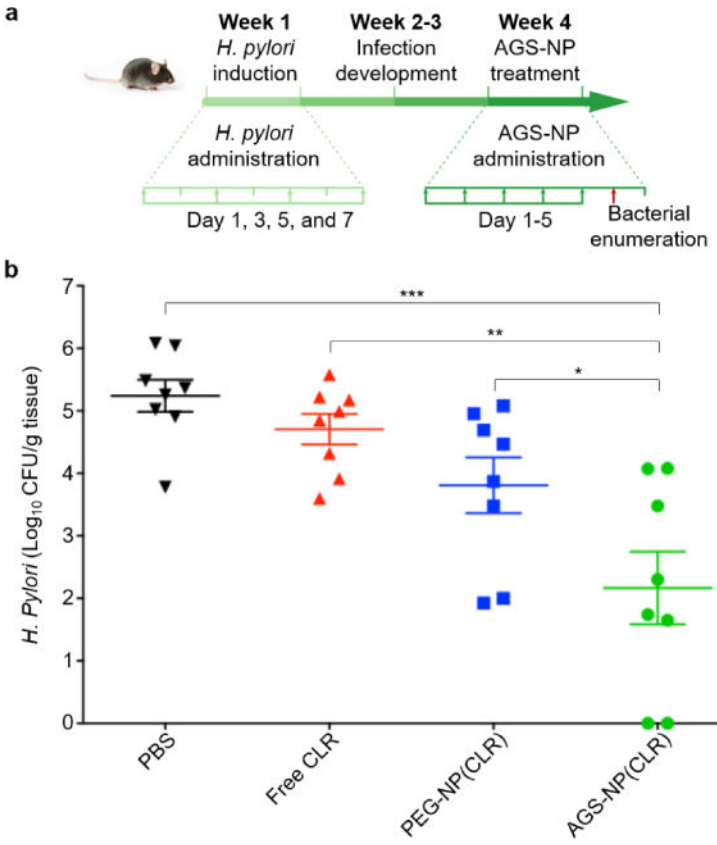

Figure 5.

In vivo anti-*H. pylori* therapeutic efficacy of AGS-NP(CLR). (a) The study protocol using a C57BL/6 mouse model of *H. pylori* infection, which includes *H. pylori* inoculation (week 1), infection development (week 2-3), and treatment (week 4). (b) Quantification of *H. pylori* bacterial burden in the stomach of infected mice treated with PBS, free CLR, PEG-NP(CLR), or AGS-NP(CLR) ($n = 6$ per group). Bars represent median values. *$P < 0.05$, **$P < 0.01$, ***$P < 0.001$.

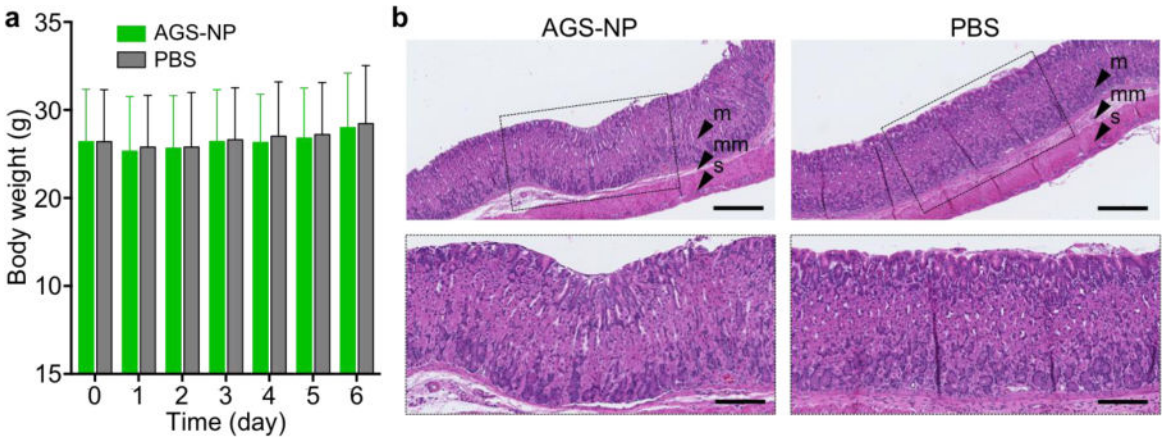

Figure 6.

Evaluation *in vivo* toxicity of AGS-NP. Uninfected mice were orally administered with the AGS-NP or PBS once daily for five consecutive days. (a) Mouse body weight log from day 0 to day 6 during study. Error bars represent the standard deviation of the mean (n = 6). (b) On day 6, mice were sacrificed and sections of the stomach were processed for histological staining with hematoxylin and eosin (H&E). Scale bars represent 250 μm in the top row and 100 μm in the bottom row). In the images on the top row, m: mucosa, mm: muscularis mucosa, and s: submucosa.